10716 *Biochemistry* **2009,** *48,* 10716–10723
DOI: 10.1021/bi901205w

BIOCHEMISTRY
including biophysical chemistry & molecular biology
Article

Substrate Redox Potential Controls Superoxide Production Kinetics in the Cytochrome *bc* Complex[†]

Jonathan L. Cape,[‡] Divesh Aidasani,[‡] David M. Kramer,[‡] and Michael K. Bowman*[,§]

[‡]*Institute of Biological Chemistry, Washington State University, 289 Clark Hall, Pullman, Washington 99164-6314, and*
[§]*Department of Chemistry, Box 870336, The University of Alabama, Tuscaloosa, Alabama 35487-0336*

Received July 15, 2009; Revised Manuscript Received October 6, 2009

ABSTRACT: The Q-cycle mechanism of the cytochrome bc_1 complex maximizes energy conversion during the transport of electrons from ubiquinol to cytochrome *c* (or alternate physiological acceptors), yet important steps in the Q-cycle are still hotly debated, including bifurcated electron transport, the high yield and specificity of the Q-cycle despite possible short-circuits and bypass reactions, and the rarity of observable intermediates in the oxidation of quinol. Mounting evidence shows that some bypass reactions producing superoxide during oxidation of quinol at the Q_o site diverge from the Q-cycle rather late in the bifurcated reaction and provide an additional means of studying initial reactions of the Q-cycle. Bypass reactions offer more scope for controlling and manipulating reaction conditions, e.g., redox potential, because they effectively isolate or decouple the Q-cycle initial reactions from later steps, preventing many complications and interactions. We examine the dependence of oxidation rate on substrate redox potential in the yeast cytochrome bc_1 complex and find that the rate limitation occurs at the level of direct one-electron oxidation of quinol to semiquinone by the Rieske protein. Oxidation of semiquinone and reduction of cyt *b* or O_2 are subsequent, distinct steps. These experimental results are incompatible with models in which the transfer of electrons to the Rieske protein is not a distinct step preceding transfer of electrons to cytochrome *b*, and with conformational gating models that produce superoxide by different rate-limiting reactions from the normal Q-cycle.

The cytochrome (cyt[1]) bc_1 (also known as Complex III or ubiquinol:cytochrome *c* oxidoreductase) and related complexes are essential energy transduction components in the respiratory and photosynthetic electron transport chains of a wide range of organisms (*1*−*4*). Its physiological role is to pump protons across the inner mitochondrial membrane to drive synthesis of ATP, but its detailed enzyme mechanism and possible roles in oxidative stress are still disputed. Our focus is on the mitochondrial cyt bc_1 complex from *Saccharomyces cerevisiae* whose dimeric functional core is illustrated in cartoon form in the left-hand side of Figure 1. Each monomer consists of three essential catalytic subunits (*2*, *5*−*8*): cyt *b*, the Rieske iron−sulfur protein (ISP), and cyt c_1. The redox-active cofactors form two distinct redox chains leading away from the quinol oxidase (Q_o) site on the positively charged side (*p*-side) of the membrane (*5*). A "low-potential chain" extends across the membrane from the Q_o site, through the cyt *b* subunit with its two *b*-type hemes (cyt b_L and cyt b_H) to the quinone reductase (Q_i) site on the negatively charged side (*n*-side) of the membrane. The "high-potential chain" consists of the Rieske FeS cluster of the ISP and the *c*-type heme of cyt c_1. This chain, on the *p*-side of the membrane, relays electrons from the Q_o site to a soluble cyt *c*.

The cyt bc_1 complex catalyzes a Q-cycle, illustrated in the left panel of Figure 1, as first proposed by Mitchell and modified extensively (*9*−*12*) as a result of the work of many researchers. In most models of the Q-cycle (*1*, *13*), QH_2 (originating from complex II in *S. cerevisiae*) binds in the Q_o site and is oxidized in the so-called "bifurcated" reaction, releasing two protons on the *p*-side of the membrane. The first QH_2 electron enters the high-potential chain at the Rieske FeS cluster. A pivoting motion of the Rieske ISP (shown as two superimposed conformations in the left panel of Figure 1) carries its FeS cluster close to cyt c_1, allowing reduction of cyt c_1, which then relays the electron to a soluble cyt *c*. Eventually, the electrons arrive at complex IV where they reduce O_2 to water.

In this model of the Q-cycle, the one-electron oxidation of QH_2 at Q_o forms a transient semiquinone (SQ) intermediate, termed SQ_o (*14*, *15*). Instead of reducing the thermodynamically favored high-potential chain a second time, SQ_o reduces cyt b_L in the low-potential chain. Electrons sent into the low-potential chain travel through cyt b_H and cyt b_L and eventually reduce a Q bound at the Q_i site. After two turnovers of the Q_o site, two electrons pass through the low-potential chain, reducing Q to QH_2 at the Q_i site, with uptake of two protons from the *n*-side of the membrane. Overall, the Q-cycle oxidizes two QH_2 molecules at Q_o, with the release of four protons on the *p*-side, and reduces one Q at Q_i with uptake of two protons from the *n*-side. The net result is a highly efficient proton pump that helps produce the transmembrane proton motive force (*pmf*) that drives ATP synthase. This complicated Q-cycle gives a stoichiometry of two protons

[†]This work was supported by National Institutes of Health Grant GM061904.

*To whom correspondence should be addressed. Phone: (205) 348-7846. Fax: (205) 348-9104. E-mail: mkbowman@as.ua.edu.

[1]Abbreviations: cyt, cytochrome; ISP, iron−sulfur protein; Q_o site, quinol oxidase site; Q_i site, quinone reductase site; FeS, two iron−two sulfur cluster in the ISP; SQ, semiquinone; SQ_o, semiquinone in Q_o; *pmf*, proton motive force; AA, antimycin A; MOA, methoxyacrylate; EPR, electron paramagnetic resonance; NMR, nuclear magnetic resonance; ESI, electrospray ionization; SOD, superoxide dismutase; K_m, Michaelis constant; V_{max}, maximum rate of reaction; K_i, inhibition constant.

 Published on Web 10/07/2009

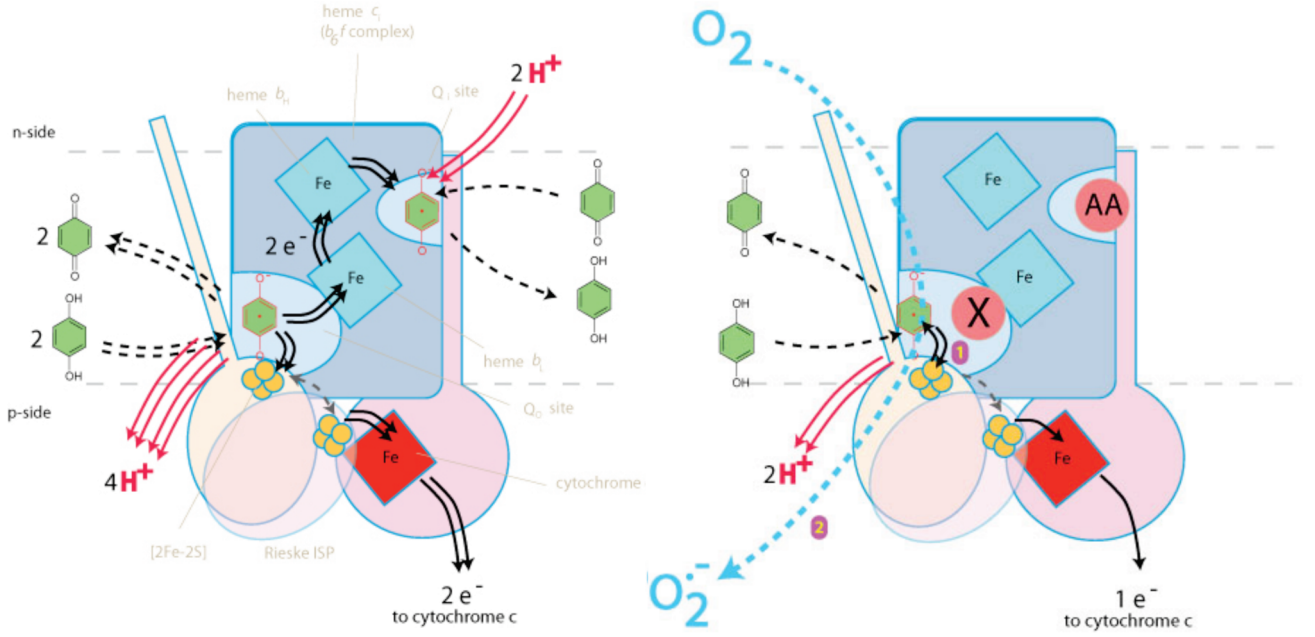

FIGURE 1: Uninhibited Q-cycle and superoxide production under partially inhibited conditions. Q-Cycle (left) showing how two turnovers at the Q_o site send two electrons through the high-potential chain to cyt *c*, and two electrons through the low-potential chain to reduce a quinone bound at the Q_i site. These reactions release four protons from QH_2 at the Q_o site (red arrows) and take up two protons by Q at the Q_i site (red arrows), resulting in a net $2H^+/e^-$ translocation stoichiometry. Blockage of the low-potential chain (right) prevents transfer of the second QH_2 electron following the initial transfer to the high-potential chain. The reactive SQ intermediate accumulates in Q_o and can reduce oxygen to form superoxide (blue arrow) or participate in other nonproductive "bypass reactions". Both panels show pivoting of the Rieske ISP, which partially gates reactions of the SQ to prevent double reduction of the high-potential chain.

translocated across the membrane per electron passed ultimately to cyt *c* in the steady state, increasing the amount of ATP synthesized per O_2 reduced (the P/O ratio) over that of a linear electron flow mechanism in which both QH_2 electrons enter the high-potential chain (*16*, *17*).

It is argued that the bifurcated electron flow also serves to "quench" the SQ_o intermediate (*18*−*27*) and prevent its reaction with O_2 to generate superoxide. Superoxide production by the Q_o site (and other reactions that "bypass" the Q-cycle) is readily observed by blocking the low-potential chain in a number of ways, including high *pmf* (*28*−*30*), high membrane potential (*30*), mutation of cyt *b* (*17*, *31*), inhibition of the Q_i site, e.g., by antimycin A (AA in the right panel of Figure 1), or inhibition of the Q_o site niche near heme b_L (proximal niche), e.g., by myxothiazole or methoxyacrylate (MOA) stilbene (X in the right panel of Figure 1) (*21*, *22*). Superoxide production at the Q_o site is hotly debated as a mitochondrial source of superoxide and other reactive oxygen species in processes such as cell signaling, aging, carcinogenesis, and metabolic diseases.

A number of reactions bypass the normal Q-cycle, reducing the efficiency of proton pumping and diverting electron flow, at least temporarily (*20*). The different bypass reactions are not mutually exclusive and might occur in combinations depending on conditions. We focus in this paper on the bypass reaction that produces superoxide during oxidation of quinol at the Q_o site because of its very intimate relation to the initial steps in the Q-cycle. Recently, superoxide production has recently been described through a very different bypass reaction that involves reduction of quinone at the Q_o site (*32*, *33*), but it will not be considered here.

Forquer et al. (*34*) recently showed that the rate-limiting step for superoxide production in the AA-inhibited mitochondrial cyt bc_1 complex is the same as for the Q-cycle, involving reduction of the Rieske FeS cluster. Thus, the Q-cycle and superoxide production share intermediates along the same, or similar, reaction pathway(s). EPR of the freeze-quenched bacterial cyt bc_1 complex suggests that this common intermediate is SQ_o (*14*, *15*). These recent results allow earlier conclusions about the order of reactions in the Q-cycle of the bacterial *Rhodobacter sphaeroides* cyt bc_1 complex (*35*) to be extended to the mitochondrial cyt bc_1 complex.

Little superoxide is generated by cyt bc_1 under normal physiological conditions. Several classes of models attempt to explain how the Q_o site steers the reaction along the Q-cycle and away from superoxide production (*14*, *15*, *34*, *35*). The experimental evidence is increasingly at odds with models in which the oxidation of QH_2 to SQ is radically different for superoxide production than for the Q-cycle, particularly the "double concerted" electron transfer mechanisms (*13*, *25*, *27*, *36*). Models that invoke conformational gating (*6*, *37*−*41*) of the Q_o site to steer electron flow are severely constrained because the same activating reaction occurs during quinol oxidation both when the putative gate functions "normally" and when it leaks, to produce superoxide (*34*).

The Q-cycle and the bypass reaction pathways must diverge at some point. With regard to this point, conflicting results have been obtained depending on reaction conditions. In contrast to Forquer et al. (*34*), Covian and Trumpower (*42*) concluded that there are different rate-limiting steps for the Q-cycle and the bypass reactions from different activation energies under pre-steady-state, non-substrate-saturated conditions. The relevance of these results to the reactions of the cyt bc_1 complex is limited until the new rate-limiting steps are identified and until it is determined which bypass reactions occur under these conditions. Consequently, we will restrict our discussion to substrate-saturated, steady-state conditions unless explicitly stated.

Important questions still remain concerning the sequence of reactions and the redox partner of the ISP in the rate-limiting step. Does quinol transfer an electron directly to the FeS cluster

thereby generating SQ_o, or is there an intervening step? What factors control the rate of superoxide production with other quinols as the substrate? Do interactions of the enzyme with particular side groups of the substrate guide the reaction and determine the products? To resolve these questions, we examine superoxide production in the yeast mitochondrial cyt bc_1 complex with a series of seven ubiquinol analogues designed to vary redox potentials and side groups on the quinol ring. One of the challenges to such work has been the limited ability to take consistent redox measurements on quinone species with the long, hydrophobic tails needed for activity. The ability to calculate these properties (*43*) now makes such a study feasible. We report here on the substrate properties that control the substrate-saturated rate of superoxide production; we identify the rate-limiting reaction, and we determine the sequence of the bifurcated electron transfer reactions.

EXPERIMENTAL PROCEDURES

Chemical Syntheses. Starting materials were purchased from Sigma-Aldrich and used without further purification, except as indicated. Substrates were purified by silica gel chromatography (0.035−0.07 mm particle size, 6 nm pore size; Acros, Geel, Belgium). Syntheses for most of these compounds, or close derivatives, have been described previously (*44*−*47*). Full details are provided as Supporting Information. Product identity was confirmed using ^1H and ^{13}C NMR spectra recorded at the Washington State University Center for NMR Spectroscopy on a Varian Mercury 300 MHz NMR spectrometer. Mass spectra were recorded on a Finnegan LCQ mass spectrometer using an ESI ionization source in negative ion mode.

Purification of the Cyt bc_1 Complex. The cyt bc_1 complex from *S. cerevisiae* was isolated from store-bought baker's yeast using the protocol of Ljungdahl et al. (*48*) with modifications (*22*). The concentration of the cyt bc_1 complex was determined by ferricyanide-ascorbate-dithionite absorbance difference spectra using published values of the extinction coefficients (*48*).

Steady-State Enzyme Turnover Measurements. Steady-state turnover rates were measured from the initial rate of cyt *c* reduction (*19*, *22*). The stigmatellin-sensitive portion of the rate is reported, so that the activity can be attributed to the Q_o site. Q-Cycle bypass is assessed in the presence of the Q_i site inhibitor, AA, at 10 μM, and the bypass rate is half the rate of cyt *c* reduction because each bypass turnover eventually transfers two electrons to cyt *c*. The rate of superoxide production was measured from the SOD-sensitive fraction of the bypass rate, recognizing that the SOD-dependent decrease in the level of cyt *c* reduction equals the level of superoxide production. The initial rates follow Michaelis−Menten kinetics. The reported V_{max} values are based on measurements at substrate concentrations several times larger than the measured K_m (Table 1).

The AA-inhibited complex is a reproducible model of other elicitors of superoxide production, such as mutation of certain Q_o and Q_i site residues (*17*, *31*, *49*, *50*), high *pmf* (*28*, *30*), or high membrane potential (*30*), in which the transfer of electrons through the low-potential chain is slowed. The use of AA also prevents reactions of the substrate at the Q_i site from influencing the measurements (see below) and eliminates the sample variability and instability noted with the use of lipid vesicles to control *pmf* or membrane potential (*30*). Yeast submitochondrial particles (data not shown) yielded similar results, ruling out artifacts from detergent solubilization or delipidization of the cyt bc_1 complex. Use of a purified complex precludes interference from other enzymes found in crude preparations or from endogenous substrates. Forquer et al. (*34*) found that purified complexes also prevented the kinetic artifacts (e.g., nonlinear or curved responses) seen in native membranes (*35*), where QH_2 concentrations were near K_m.

Table 1: Kinetic Parameters for Steady-State Turnover of the AA-Inhibited Cyt bc_1 Complex[a]

substrate	K_m	V_{max}(bypass)	f_{SOP}	V_{max}(SO)	K_i(C)	K_i(NC)	ΔE_m
1	23	2.4	0.68	1.6	2.1	−	−0.060
2	25	2.2	−	1.1−1.7	11.8	5.8	−0.019
3	5	0.6	0.66	0.4	−	−	−
4	>150	7.5	0.71	5.3	−	−	−
5	9	27	0.55	15.1	4.4	7.1	−0.018
6	35	*80*	−	*40*−*60*	−	−	−
7	30	*199*	0.51	*101*	26.2	36.8	−0.003

[a] f_{SOP} is the fraction of Q-cycle bypass reactions resulting in superoxide production derived from the superoxide dismutase sensitivity of cyt *c* reduction in the AA-inhibited complex. Product inhibition constants K_i for a mixed inhibition model are for uninhibited steady-state turnover driven by decyl-ubiquinol. K_m and K_i are reported in units of micromolar. Rates of quinol oxidation are given in units of inverse seconds from total bypass reactions [V_{max}(bypass)] and from superoxide-producing bypass reactions [V_{max}(SO)]. In two cases, V_{max}(SO) could not be measured but is estimated as a range: 0.5−0.75 V_{max}(bypass) covering the range of measured f_{SOP} values. Rates noted in italics were measured by stopped-flow methods. The shifts in redox potential for the Q/QH_2 couple based on measured values of K_m and the competitive K_i are reported in volts.

The fast initial rates of some bypass reactions were verified by stopped-flow techniques, measuring the rate of cyt *c* reduction, as described above (see Table 1). The substrate concentrations used in stopped-flow experiments were well in excess of the steady-state K_m values, resulting in rates that were independent of substrate concentration. Competition assays between non-native Q-species and the native substrate analogue (**3**) were used to estimate the K_i of the non-native Q species and were analyzed using a mixed competitive inhibition model (*51*) with simultaneous fitting of substrate titration curves over a range of quinone concentrations, holding the uninhibited K_m and V_{max} values constant. Shifts in the Q/QH_2 potential from differential Q/QH_2 binding were estimated from the ratio of competitive K_i/K_m values. In some cases, decyl-ubiquinol was used in place of **3** (differing by one carbon in the tail) with identical results.

Thermodynamic Properties of QH_2 Substrates. The estimation of free energy changes (ΔG) for reactions involving SQ in the Q_o site requires accurate one- and two-electron redox potentials and pK_a values for all the Q, SQ, and QH_2 species bound to the protein at the Q_o site. Measurement of many of the required quantities has not been experimentally possible. However, for the series of closely related *p*-benzoquinone derivatives used here, the redox potentials and pK_a values in the Q_o site should be offset from the corresponding aqueous solution values by a similar amount if there are no strong specific interactions affecting some molecules in the series much more than the others. The ΔG for a reaction in the protein should be shifted by a similar amount. Thus, the change in the free energy of reaction, $\Delta\Delta G$, for different substrate analogues in this series should be similar whether estimated using the inaccessible values in the protein or the values in aqueous solution.

The use of aqueous properties has its own challenges. Aqueous redox potentials from cyclic voltammetric measurements are not reliable for many lipophilic quinone species (*43*, *52*, *53*). Moreover, the reduction potential for the Q to $Q^{\bullet-}$ reaction (or the oxidation of QH_2 to $QH^{\bullet}$ or $Q^{\bullet-}$) is nearly impossible to measure

Table 2: Calculated Aqueous Redox Potentials and pK_a Values for SQ Species, Estimated K_s Values, and SQ/QH_2 Potentials for Protonated and Deprotonated SQ Species[a]

substrate	$E(Q/QH_2)$	$E(Q/Q^{\bullet-})$	pK_{aSQ}	log K_S	$E(QH^{\bullet}/QH_2)$	$E(Q^{\bullet-}/QH_2)$
1	0.178	0.087	4.70	−9.66	0.463	0.269
2	0.112	−0.088	5.33	−12.09	0.469	0.312
3	0.122	−0.078	5.35	−12.05	0.478	0.322
4	−0.018	−0.156	4.86	−10.93	0.305	0.12
5	−0.003	−0.072	5.19	−7.94	0.231	0.066
6	−0.067	−0.148	4.79	−9.14	0.203	0.014
7	−0.108	−0.052	5.10	−3.89	0.007	−0.164

[a] K_S is defined as the the equilibrium constant for comproportionation of Q and QH_2 to form $2QH^{\bullet}$. All potentials and equilibrium constants are adjusted to the experimental conditions of pH 8.0. Redox potentials are given in volts vs the standard hydrogen electrode.

reliably by experiment in aqueous solution because of the disproportionation of the semiquinone species in the solutions. Fortunately, there is sufficient experimental data to support the calculation of aqueous redox potentials and pK_a values in this series of substrate analogues. We use procedures that predict reasonably accurate aqueous redox potentials across a series of homologous water-soluble quinone species (*43*), similar to "benchmarking" approaches used successfully in other cases to predict accurate redox potentials and pK_a values (*54*, *55*). The computed values are summarized in Table 2 with full details in the Supporting Information.

RESULTS

Kinetics of Superoxide Production in AA-Inhibited Complexes. The apparent Michaelis constant (K_m) and the maximum velocity of superoxide production (V_{max}) were determined for substrates **1**−**7** (Scheme 1 and Table 1). The K_m values reflect the coefficient for partitioning of each substrate analogue into the detergent or membrane and the apparent binding constant at the Q_o site. The K_m values for all substrate analogues lie in the range of 5−35 μM except for **4**, which has solubility problems and a large apparent K_m of ∼150 μM.

For several substrates, the AA-inhibited turnover assays slowed markedly as the product Q accumulated. Such behavior has been observed for other non-native substrates (*19*, *45*) and indicates product inhibition; that is, the oxidized substrate binds more tightly to Q_o than the substrate itself. Product inhibition implies that the Q/QH_2 redox potential shifts to more negative values when bound at Q_o. To measure those shifts, binding constants for the oxidized substrates at Q_o were estimated from competition assays on uninhibited, steady-state turnover driven by decyl-ubiquinol. The data were analyzed with mixed competition kinetics with competitive inhibition considered to be binding of the quinol at the Q_o site and the noncompetitive inhibition as binding of Q at a site distinct from the Q_o binding pocket, probably the Q_i site. The K_i values were significant for only four substrates, and the calculated shifts in the redox potential [E_m(Q/QH_2)] based on the K_m and competitive K_i values range from −0.003 to −0.060 V, less than the uncertainty in calculated redox potential and much less than the range of potentials for **1**−**7**.

Superoxide Production Rates Are Related to the Potentials for SQ Formation. The V_{max} for superoxide production varies by more than 2 orders of magnitude for substrates **1**−**7** and depends strongly on the relative redox potential for the one-electron oxidation of **1**−**7** (Figure 2). Remarkably, these data plotted as a function of the shift in the oxidation potential of QH_2 relative to UQH_2 form a smooth extension of the data of Forquer et al. (*34*) plotted as a function of the reduction potential shifts of the Rieske ISP (as varied by site-directed mutagenesis in *S. cerevisiae*). The reaction rate varies consistently with changes in the redox potential of the QH_2/ISP couple whether the redox potential of the substrate or of the ISP is changed. These combined data show that the rate-limiting step for superoxide generation depends on the redox potential for the one-electron reduction of the Rieske ISP by substrate.

The relation is equally strong whether we consider the redox potential for the $QH^{\bullet}/QH_2$ or $Q^{\bullet-}/QH_2$ couples (Figure 2). The semiquinones of **1**−**7** all have similar pK_a values (Table 1), which forces the potentials for oxidation of QH_2 to $QH^{\bullet}$ or $Q^{\bullet-}$ to shift by similar amounts. Notably, there is no correlation between the rate of superoxide production and the potential for the second electron transfer (Figure 3), indicating that the oxidation of SQ_o is not rate-limiting for the production of superoxide.

Scheme 1: Synthetic QH_2 Substrates[a]

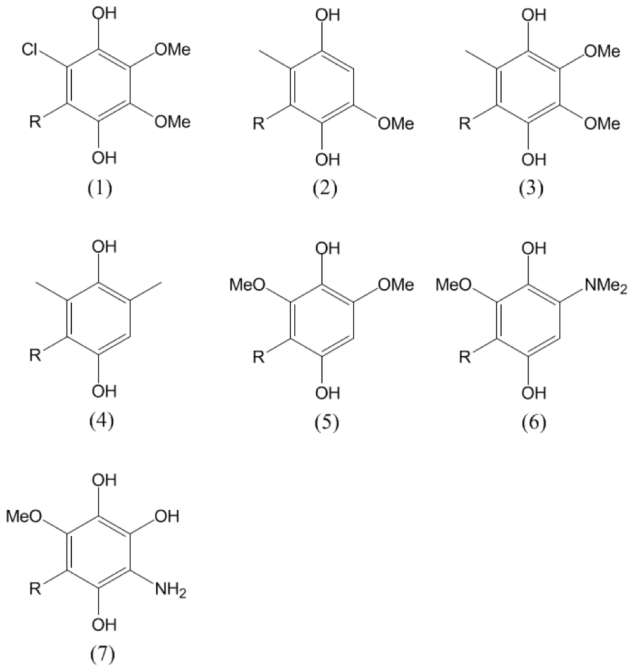

[a] R denotes the *n*-undecyl group ($C_{11}H_{23}$).

DISCUSSION

Specific Molecular Interactions Do Not Have Large Effects on Superoxide Production. Alterations to the QH_2 substrate of the Q_o site can cause the cyt bc_1 complex to produce superoxide at rates exceeding that of normal Q-cycle turnover (∼100 s^{-1}) [Figure 2 and previous work (*19*)]. Altering the substrate could elicit rapid superoxide production by altering specific interactions between the binding site and the substrate that are crucial for steering or gating the reaction into products, or by changing the driving force for formation or subsequent reaction of SQ_o. This work was designed to distinguish between these possibilities by probing superoxide production with a homologous series of synthetic substrate analogues.

The substrate analogues were selected, in part, to vary the side groups on the benzoquinone ring available to participate in specific interactions with the Q_o site. Aside from the obvious effects of ring substituents on redox potentials (see below), there is no discernible relation between superoxide production and the

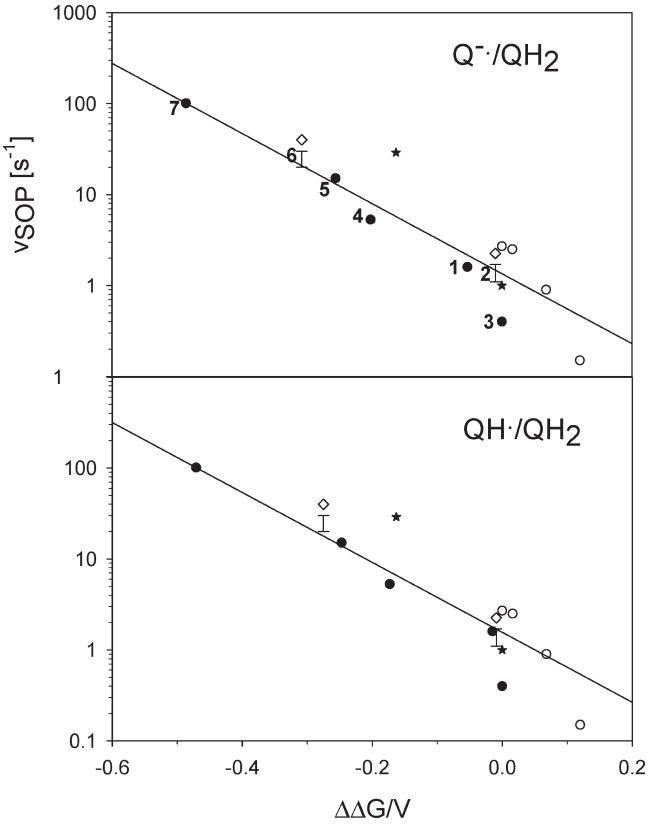

FIGURE 2: V_{max} for superoxide production, v_{SOP}, in micromoles of superoxide per micromole of cyt bc_1 per second measured with saturating amounts of substrate analogue and corresponding to V_{max}. Rates are plotted as a function of the shift ($\Delta\Delta G$) in oxidation potential for substrate analogues [$QH_2/Q^{\bullet -}$ (top) and $QH_2/QH^{\bullet}$ (bottom)] or reduction potential for the Rieske ISP: (●) v_{SOP} for substrate analogues from Table 1 (the analogue is indicated by number to the left of the symbol), (○) v_{SOP} for Rieske ISP mutants from Forquer et al. (*34*) measured using the Amplex Red assay, (∗) v_{SOP} for substrate analogues UQ_3 and RQ_3 from Cape et al. (*19*), and (◇) V_{max} for total bypass in micromoles of substrate analogue oxidized per micromole of cyt bc_1 per second for **2** and **6** with the typical v_{SOP} range indicated directly below by "error" bars.

position or type of ring substituent in **1**−**7**. The quinol OH groups and the hydrocarbon tail are certainly necessary for activity, yet groups at other positions can change the V_{max} by 2 orders of magnitude! The V_{max} for superoxide production in the AA-inhibited complex is little affected by which hydrophobic tail is attached, with undecylubiquinol, **3**, decylubiquinol (*34*), and ubiquinol-3 (*19*) giving essentially equal rates. The position and identity of individual chloro, methyl, methoxy, or amino side groups also are not decisive in determining the V_{max} for superoxide production [except through their overall influence on the redox potential (see below)]. The rate of electron transfer from a substrate analogue in this series bound at the Q_o site is not controlled by the physical structure of the substrate analogue.

Superoxide Production Rates Are Controlled by the Driving Force for SQ_o Formation. The substrate analogues were also selected to provide large variations in both Q/QH_2 redox potential and semiquinone stability constant, K_s (Table 2). The large scatter in K_s means that the potential or driving force for the first electron transfer does not track the potential for the second electron transfer (from SQ_o to O_2) and makes it possible to distinguish between the first and second electron transfer reactions. The V_{max} for superoxide production increases as the quinol becomes a better one-electron reducing agent and as the Rieske

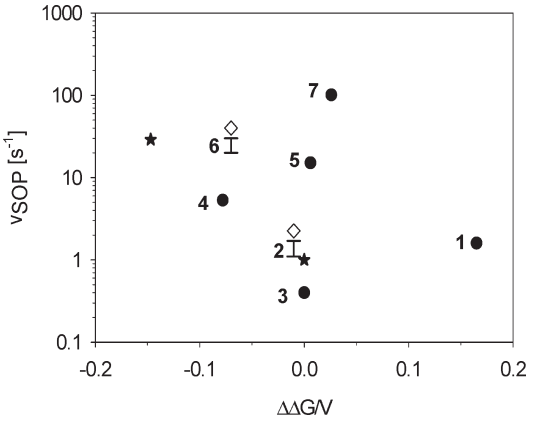

FIGURE 3: V_{max} for superoxide production, v_{SOP}, in micromoles of superoxide per micromole of cyt bc_1 per second measured with saturating amounts of substrate analogue. Rates are plotted as a function of the shift in oxidation potential for substrate analogues for QH_2/Q couples. Symbols are the same as in Figure 2A.

ISP becomes easier to reduce (*34*) (Figure 2). That is, the rate of the reaction depends on the driving force for the one-electron oxidation of the substrate by the Rieske ISP but not on the driving force for the oxidation of SQ_o. Thus, the rate-limiting step with saturating substrate concentrations in superoxide production is the direct, one-electron oxidation of QH_2 by the ISP to produce SQ_o and reduced ISP. Because the activation energy with the natural substrate (*34*) for this step is the same as for the normal Q-cycle, the first electron transfer step in the bifurcated oxidation of quinol in the cyt bc_1 complex must also be the direct, one-electron oxidation of QH_2 by the ISP. Covian and Trumpower (*42*) recently reported that the first electron transfer step is no longer the rate-limiting step at less than saturating substrate concentrations. They concluded that the rate limitation occurs at a different step for normal turnover than for the bypass reactions that occur under their conditions. That report did not determine where the rate limitation moved in the complicated, multistep reaction pathway of the cyt bc_1 complex or whether the bypass reactions under those new conditions result in superoxide production.

Superoxide Is Produced by SQ. Figures 2 and 3 clearly show that the rate-limiting step for superoxide production is the first electron transfer. But what is the immediate source of the electron to convert O_2 into superoxide: the reduced Rieske ISP, the reduced cyt b_L, or SQ_o? It is not likely the Rieske ISP. In contrast to the FeS cluster in Complex I, the reduced Rieske ISP is rather stable in air-saturated solutions either as part of the cyt bc_1 complex or as the purified protein because of its unusually high redox potential (~0.275 V at pH 7.0) (*56*). Its ability to reduce oxygen is incapable of supporting the measured superoxide production rates. Furthermore, measurements of bypass reactions in the cyt bc_1 complex find that at least one electron per quinol makes it through the high-potential chain (*21*, *22*), safely passing through the Rieske ISP. An electron that enters the high-potential chain at the Rieske ISP apparently is not easily diverted to superoxide.

The electron to convert O_2 to superoxide therefore must come from SQ_o, but its path to O_2 is not obvious. Electron transfer from SQ_o through heme b_L or the low-potential chain to produce superoxide is one possibility. The proximal niche inhibitors myxothiazole and MOA stilbene (*21*, *22*) prevent electrons from entering the low-potential chain yet elicit substantial amounts of

such superoxide from the cyt bc_1 complex. Muller et al. (*21*) showed that the V_{max} for superoxide production in the presence of proximal niche inhibitors is roughly half that of AA-inhibited complexes. This provides a clear demonstration that reduced cyt b_L is not an essential precursor to superoxide because proximal niche inhibitors prevent electrons from entering the low-potential chain and reducing cyt b_L. Moreover, when electrons can enter the low-potential chain, as with AA inhibition, the steady-state accumulation of electrons on cyt b_L ought to cause superoxide production at rates proportional to the amount of reduced cyt b_L. Available data do not support this prediction (*19*); very reducing substrates such as rhodoquinol generate steady-state levels of reduced cyt *b* similar to that of ubiquinol even though superoxide production rates differ by ~2 orders of magnitude. Thus, the low-potential chain does not appear to be able to pass electrons efficiently from SQ_o to superoxide.

SQ_o is the only remaining plausible source of the electron for superoxide production, and SQ_o must therefore be considered the last known predecessor of superoxide. However, there are little direct data to indicate whether SQ_o reacts in the Q_o site to produce superoxide or after escape from the Q_o site.

Recent studies of superoxide production during "semireverse" electron flow (*32*, *33*) conclude that under extreme conditions, electron flow in the low-potential chain can be reversed, with electrons flowing from the Q_i site to the Q_o site, to reduce quinone in the Q_o site to SQ_o and then producing superoxide. That route to superoxide production supports our results that SQ_o is the last known precursor to superoxide.

Superoxide Production Shares Intermediates with the Q-Cycle. Superoxide production rates at saturating substrate concentrations are related to shifts in redox potential of both the Rieske ISP and the quinol substrate (Figure 2). The relationship can be summarized following Crofts et al. (*23*), based on Marcus theory as

$$v \propto \exp\left(-\frac{\Delta\Delta G}{RT}\right) \propto \exp\left[-F\frac{E(\mathrm{SQ/QH_2}) - E(\mathrm{ISP_{ox}/ISP_{red}})}{RT}\right]$$

This equation has been experimentally tested by variation of the ISP redox potential for normal Q-cycle turnover (*23*, *34*) and for superoxide production (*23*). We now find that it holds when the redox potential of the substrate is varied. Thus, the free energy change for the one-electron transfer from substrate to the ISP predicts the rate of superoxide production. This indicates that the rate-limiting step for superoxide production is the one-electron transfer reaction to produce SQ_o (either as the neutral radical or as the radical anion) and reduced ISP. The activation energies at saturating substrate concentrations are the same for superoxide production and for oxidation of quinol in the Q-cycle (*34*), indicating the same rate-limiting step in both processes. The paths then diverge at SQ_o or soon thereafter as proposed previously (*23*, *34*).

The initial electron transfer is thought to occur in a hydrogen-bonded complex between quinol and a histidine ligand of the FeS cluster (*23*, *32*, *34*, *57*). In such a "contact ion pair", back electron transfer should be rapid. A distinct SQ_o would appear only after the contact ion pair moves apart and back electron transfer slows dramatically, to kinetically "trap" SQ_o so that it reacts with O_2 or proceeds along the Q-cycle. The motion of the ISP headgroup to carry its FeS cluster to cyt c_1 is the obvious way for the contact ion pair to dissociate and to terminate the electron transfer step. This view predicts that blocking movement of the ISP would prevent formation of SQ_o and superoxide. Indeed, Borek et al. (*32*) reported no superoxide production in the double alanine insertion mutant of the ISP, where ISP movement is blocked (*56*). This observation was explained by a gating mechanism in which "the structural changes that occur in the Q_o site upon movement of FeS" "act to transiently 'open' the Q_o site for the reaction with oxygen" (*32*). The "opening" of this gate is perhaps best viewed in a general sense in which a fully reactive SQ_o is not formed until the ISP has moved away from Q_o.

CONCLUSION

Mounting evidence shows that some of the bypass reactions, particularly those producing superoxide during oxidation of quinol at the Q_o site, diverge from the Q-cycle rather late in the bifurcated reaction. Consequently, bypass reactions provide an additional means of studying the initial reactions of the Q-cycle as demonstrated here. There is more scope for controlling and manipulating reaction conditions, e.g., varying redox potential, because the bypass reactions effectively isolate or decouple the initial reactions in the Q-cycle from later steps, preventing many complications and interactions. We used that approach here to examine the dependence of oxidation rate on the redox potential and structure of the substrate. We find that the direct one-electron oxidation of QH_2 by the Rieske ISP produces a semiquinone during oxidation of quinol at the Q_o site in the Q-cycle and in superoxide production. The oxidation of the semiquinone and the reduction of cyt *b* or O_2 are subsequent steps, distinct from the rate-limiting step. The production of superoxide whether through the oxidation of quinol in the Q_o site studied here or through the reduction of quinone in the Q_o site by reversed electron flow (*32*, *33*) involves the generation of SQ_o which is the last known precursor to superoxide. At lower substrate concentrations, other reactions become rate-limiting and detailed measurements of carefully designed mutants and substrate analogues or of kinetic isotope effects can make substantial contributions to determining the entire reaction network.

These experimental results reported here are incompatible (1) with models for cyt bc_1 in which transfer of electrons to the high-potential chain is not a distinct step preceding transfer of electrons to the low-potential chain and (2) with conformational gating models that would produce superoxide by a very different set of reactions compared to the normal Q-cycle.

ACKNOWLEDGMENT

We acknowledge many useful discussions, in particular with Wolfgang Nitschke, Fevzi Daldal, Christopher Moser, P. Leslie Dutton, Antony R. Crofts, and Isaac Forquer. We also thank Daniel Vasseo and Michael Jourdes for their technical assistance.

SUPPORTING INFORMATION AVAILABLE

Syntheses of the substrate analogues used in this study and the details of the estimation of redox potentials. This material is available free of charge via the Internet at http://pubs.acs.org.

REFERENCES

1. Crofts, A. R. (2004) The cytochrome bc_1 complex: Function in the context of structure. *Annu. Rev. Physiol. 66*, 689–733.
2. Berry, E. A., Guergova-Kuras, M., Huang, L. S., and Crofts, A. R. (2000) Structure and function of cytochrome *bc* complexes. *Annu. Rev. Biochem. 69*, 1005–1075.
3. Schutz, M., Brugna, M., Lebrun, E., Baymann, F., Huber, R., Stetter, K. O., Hauska, G., Toci, R., Lemesle-Meunier, D., Tron, P., Schmidt,

C., and Nitschke, W. (2000) Early evolution of cytochrome *bc* complexes. *J. Mol. Biol. 300*, 663–675.
4. Nitschke, W., Kramer, D. M., Riedel, A., and Liebl, U. (1995) From naphtho- to benzoquinones—(R)evolutionary reorganizations of electron transfer chains. In Photosynthesis: From Light to Biosphere (Mathis, P., Ed.) pp 945−948, Kluwer Academic Publishers, Dordrecht, The Netherlands.
5. Iwata, S., Lee, J. W., Okada, K., Lee, J. K., Iwata, M., Rasmussen, B., Link, T. A., Ramaswamy, S., and Jap, B. K. (1998) Complete structure of the 11-subunit bovine mitochondrial cytochrome bc_1 complex. *Science 281*, 64–71.
6. Crofts, A. R., Berry, E. A., Kuras, R., Guergova-Kuras, M., Hong, S., and Ugulava, N. B. (1999) Structures of the bc1 complex reveal dynamic aspects of mechanism. In Photosynthesis: Mechanisms and Effects (Garab, G., Ed.) pp 1481−1486, Kluwer Academic Publishers, Dordrecht, The Netherlands.
7. Hunte, C., Palsdottir, H., and Trumpower, B. L. (2003) Protonmotive pathways and mechanisms in the cytochrome bc_1 complex. *FEBS Lett. 545*, 39–46.
8. Esser, L., Quinn, B., Li, Y. F., Zhang, M. Q., Elberry, M., Yu, L., Yu, C. A., and Xia, D. (2004) Crystallographic Studies of Quinol Oxidation Site Inhibitors: a Modified Classification of Inhibitors for the Cytochrome bc_1 Complex. *J. Mol. Biol. 341*, 281–302.
9. Mitchell, P. (1975) The protonmotive Q cycle: A general formulation. *FEBS Lett. 59*, 137–139.
10. Crofts, A. R., Shinkarev, V. P., Kolling, D. R. J., and Hong, S. J. (2003) The Modified Q-Cycle Explains the Apparent Mismatch Between the Kinetics of Reduction of Cytochromes c_1 and b_H in the bc_1 Complex. *J. Biol. Chem. 278*, 36191–36201.
11. Crofts, A. R., and Wang, Z. (1989) How rapid are the internal reactions of the ubiquinol: Cytochrome c_2 oxidoreductase? *Photosynth. Res. 22*, 69–87.
12. Crofts, A. R., and Wraight, C. A. (1983) The Electrochemical Domain of Photosynthesis. *Biochim. Biophys. Acta 726*, 149–185.
13. Berry, E. A., and Huang, L. S. (2003) Observations Concerning the Quinol Oxidation Site of the Cytochrome bc_1 Complex. *FEBS Lett. 555*, 13–20.
14. Cape, J. L., Bowman, M. K., and Kramer, D. M. (2007) A semiquinone intermediate generated at the Q_o site of the cytochrome bc_1, complex: Importance for the Q-cycle and superoxide production. *Proc. Natl. Acad. Sci. U.S.A. 104*, 7887–7892.
15. Zhang, H. B., Osyczka, A., Dutton, P. L., and Moser, C. C. (2007) Exposing the complex III Q_o semiquinone radical. *Biochim. Biophys. Acta 1767*, 883–887.
16. Schultz, B. E., and Chan, S. I. (2001) Structures and proton-pumping strategies of mitochondrial respiratory enzymes. *Annu. Rev. Biophys. Biomol. Struct. 30*, 23–65.
17. Wenz, T., Hellwig, P., MacMillan, F., Meunier, B., and Hunte, C. (2006) Probing the role of E272 in quinol oxidation of mitochondrial complex III. *Biochemistry 45*, 9042–9052.
18. Cape, J. L., Bowman, M. K., and Kramer, D. M. (2006) Understanding the Cytochrome *bc* Complexes by What They Don't Do. The Q-Cycle at 30. *Trends Plant Sci. 11*, 46–55.
19. Cape, J. L., Strahan, J. R., Lenaeus, M. J., Yuknis, B. A., Trieu, T. L., Shepherd, J. N., Bowman, M. K., and Kramer, D. M. (2005) The Respiratory Substrate Rhodoquinol Induces Q-cycle Bypass Reactions in the Yeast Cytochrome bc_1 Complex: Mechanistic and Physiological Implications. *J. Biol. Chem. 280*, 34654–34660.
20. Kramer, D. M., Roberts, A. G., Muller, F. L., Cape, J., and Bowman, M. K. (2004) Q-cycle Bypass Reactions at the Q_o site of the Cytochrome bc_1 (and Related) Complexes. *Methods Enzymol. 382*, 21–45.
21. Muller, F. L., Roberts, A. G., Bowman, M. K., and Kramer, D. M. (2003) Architecture of the Q_o site of the cytochrome bc_1 complex probed by superoxide production. *Biochemistry 42*, 6493–6499.
22. Muller, F., Crofts, A. R., and Kramer, D. M. (2002) Multiple Q-cycle bypass reactions at the Q_o site of the cytochrome bc_1 complex. *Biochemistry 41*, 7866–7874.
23. Crofts, A. R., Lhee, S., Crofts, S. B., Cheng, J., and Rose, S. (2006) Proton pumping in the bc_1 complex: A new gating mechanism that prevents short circuits. *Biochim. Biophys. Acta 1757*, 1019–1034.
24. Mulkidjanian, A. Y. (2005) Ubiquinol oxidation in the cytochrome bc_1 complex: Reaction mechanism and prevention of short-circuiting. *Biochim. Biophys. Acta 1709*, 5–34.
25. Osyczka, A., Moser, C. C., and Dutton, P. L. (2005) Fixing the Q cycle. *Trends Biochem. Sci. 30*, 176–182.
26. Rich, P. R. (2004) The quinone chemistry of BC complexes. *Biochim. Biophys. Acta. 1658* (Suppl. S), 32.
27. Osyczka, A., Moser, C. C., Daldal, F., and Dutton, P. L. (2004) Reversible Redox Energy Coupling in Electron Transfer Chains. *Nature 427*, 607–612.
28. Shinkarev, V. P., Crofts, A. R., and Wraight, C. A. (2001) The electric field generated by photosynthetic reaction center induces rapid reversed electron transfer in the bc_1 complex. *Biochemistry 40*, 12584–12590.
29. Tahara, E. B., Navarete, F. D. T., and Kowaltowski, A. J. (2009) Tissue-, substrate-, and site-specific characteristics of mitochondrial reactive oxygen species generation. *Free Radical Biol. Med. 46*, 1283–1297.
30. Rottenberg, H., Covian, R., and Trumpower, B. L. (2009) Membrane potential greatly enhances superoxide generation by the cytochrome bc_1 complex reconstituted into phospholipid vesicles. *J. Biol. Chem. M109*, 017376.
31. Fisher, N., Castleden, C. K., Bourges, I., Brasseur, G., Dujardin, G., and Meunier, B. (2004) Human Disease-Related Mutations in Cytochrome *b* Studied in Yeast. *J. Biol. Chem. 279*, 12951–12958.
32. Borek, A., Sarewicz, M., and Osyczka, A. (2008) Movement of the Iron-Sulfur Head Domain of Cytochrome bc_1 Transiently Opens the Catalytic Q_o Site for Reaction with Oxygen. *Biochemistry 47*, 12365–12370.
33. Drose, S., and Brandt, U. (2008) The Mechanism of Mitochondrial Superoxide Production by the Cytochrome bc_1 Complex. *J. Biol. Chem. 283*, 21649–21654.
34. Forquer, I., Covian, R., Bowman, M. K., Trumpower, B. L., and Kramer, D. M. (2006) Similar transition states mediate the Q-cycle and superoxide production by the cytochrome bc_1 complex. *J. Biol. Chem. 281*, 38459–38465.
35. Hong, S. J., Ugulava, N., Guergova-Kuras, M., and Crofts, A. R. (1999) The Energy Landscape for Ubihydroquinone Oxidation at the Q_o Site of the bc_1 Complex in *Rhodobacter sphaeroides*. *J. Biol. Chem. 274*, 33931–33944.
36. Trumpower, B. L. (2002) A Concerted, Alternating Sites Mechanism of Ubiquinol Oxidation by the Dimeric Cytochrome bc_1 Complex. *Biochim. Biophys. Acta 1555*, 166–173.
37. Lange, C., and Hunte, C. (2002) Crystal structure of the yeast cytochrome bc_1 complex with its bound substrate cytochrome *c*. *Proc. Natl. Acad. Sci. U.S.A. 99*, 2800–2805.
38. Darrouzet, E., Valkova-Valchanova, M., Moser, C. C., Dutton, P. L., and Daldal, F. (2000) Uncovering the [2Fe2S] Domain Movement in Cytochrome bc_1 and its Implications for Energy Conversion. *Proc. Natl. Acad. Sci. U.S.A. 97*, 4567–4572.
39. Darrouzet, E., Valkova-Valchanova, M., Ohnishi, T., and Daldal, F. (1999) Structure and function of the bacterial bc_1 complex: Domain movement, subunit interactions, and emerging rationale engineering attempts. *J. Bioenerg. Biomembr. 31*, 275–288.
40. Crofts, A. R. (2006) The bc1 Complex: What is There Left to Argue About? In Biophysical and Structural Aspects of Bioenergetics (Wikstrom, M., Ed.) pp 123−155, Royal Society of Chemistry, Cambridge, U.K.
41. Iwata, M., Bjorkman, J., and Iwata, S. (1999) Conformational change of the Rieske [2Fe-2S] protein in cytochrome bc_1 complex. *J. Bioenerg. Biomembr. 31*, 169–175.
42. Covian, R., and Trumpower, B. L. (2009) The Rate-limiting Step in the Cytochrome bc_1 Complex (Ubiquinol-Cytochrome c Oxidoreductase) Is Not Changed by Inhibition of Cytochrome *b*-dependent Deprotonation: Implications for the Mechanism of ubiquinol Oxidation at Center P of the bc_1 Complex. *J. Biol. Chem. 284*, 14359–14367.
43. Cape, J. L., Bowman, M. K., and Kramer, D. M. (2006) Computation of the redox and protonation properties of quinones: Towards the prediction of redox cycling natural products. *Phytochemistry 67*, 1781–1788.
44. Folkers, K., Catlin, J. C., and Daves, G. D. (1971) Coenzyme Q. 124. New substituted 2,3-dimethoxy-1,4-benzoquinones as inhibitors of coenzyme Q systems. *J. Med. Chem. 14*, 45–48.
45. Gu, L. Q., Yu, L., and Yu, C. A. (1990) Effect of Substituents of the Benzoquinone Ring on Electron-Transfer Activities of Ubiquinone Derivatives. *Biochim. Biophys. Acta 1015*, 482–492.
46. Keegstra, E. M. D., Huisman, B. H., Paardekooper, E. M., Hoogesteger, F. J., Zwikker, J. W., Jenneskens, L. W., Kooijman, H., Schouten, A., Veldman, N., and Spek, A. L. (1996) 2,3,5,6-Tetraalkoxy-1,4-benzoquinones and structurally related tetraalkoxy benzene derivatives: Synthesis, properties and solid state packing motifs. *J. Chem. Soc., Perkin Trans. 2*, 229–240.
47. Gu, L. Q., Yu, L., and Yu, C. A. (1989) A ubiquinone derivative that inhibits mitochondrial cytochrome bc_1 complex but not chloroplast cytochrome b_6f complex activity. *J. Biol. Chem. 264*, 4506–4512.

48. Ljungdahl, P. O., Pennoyer, J. D., Robertson, D. E., and Trumpower, B. L. (1987) Purification of highly active cytochrome bc_1 complexes from phylogenetically diverse species by a single chromatographic procedure. *Biochim. Biophys. Acta 891*, 227–241.
49. Fisher, N., Bourges, I., Hill, P., Brasseur, G., and Meunier, B. (2004) Disruption of the interaction between the Rieske iron-sulfur protein and cytochrome *b* in the yeast bc_1 complex owing to a human disease-associated mutation within cytochrome *b*. *Eur. J. Biochem. 271*, 1292–1298.
50. Wenz, T., Covian, R., Hellwig, P., MacMillan, F., Meunier, B., Trumpower, B. L., and Hunte, C. (2007) Mutational analysis of cytochrome *b* at the ubiquinol oxidation site of yeast complex III. *J. Biol. Chem. 282*, 3977–3988.
51. Fresht, A. (1977) Enzyme Structure and Mechanism, W. H. Freeman, San Francisco.
52. Marchal, D., Boireau, W., Laval, J. M., Moiroux, J., and Bourdillon, C. (1997) An electrochemical approach of the redox behavior of water insoluble ubiquinones or plastoquinones incorporated in supported phospholipid layers. *Biophys. J. 72*, 2679–2687.
53. Michalkiewicz, S. (2007) Cathodic reduction of coenzyme Q_{10} on glassy carbon electrode in acetic acid-acetonitrile solutions. *Bioelectrochemistry 70*, 495–500.
54. Baik, M. H., and Friesner, R. A. (2002) Computing redox potentials in solution: Density functional theory as a tool for rational design of redox agents. *J. Phys. Chem. A 106*, 7407–7412.
55. Fu, Y., Liu, L., Wang, Y. M., Li, J. N., Yu, T. Q., and Guo, Q. X. (2006) Quantum-chemical predictions of redox potentials of organic anions in dimethyl sulfoxide and reevaluation of bond dissociation enthalpies measured by the electrochemical methods. *J. Phys. Chem. A 110*, 5874–5886.
56. Cooley, J. W., Roberts, A. G., Bowman, M. K., Kramer, D. M., and Daldal, F. (2004) The Raised Midpoint Potential of the [2Fe2S] Cluster of Cytochrome bc_1 Is Mediated by Both the Q_o Site Occupants and the Head Domain Position of the Fe-S Protein Subunit. *Biochemistry 43*, 2217–2227.
57. Cape, J. L., Bowman, M. K., and Kramer, D. M. (2005) Reaction Intermediates of Quinol Oxidation in a Photoactivatable System That Mimics Electron Transfer in the Cytochrome bc_1 Complex. *J. Am. Chem. Soc. 127*, 4208–4215.